ISIJ International, Vol. 52 (2012), No. 12, pp. 2200–2204

Chemical Composition and Morphology of M_7C_3 Eutectic Carbide in High Chromium White Cast Iron Alloyed with Vanadium

Mirjana FILIPOVIC,* Endre ROMHANJI and Zeljko KAMBEROVIC

Department of Metallurgical Engineering, Faculty of Technology and Metallurgy, University of Belgrade, Karnegijeva 4, Belgrade, 11120 Serbia.

(*Received on May 5, 2012; accepted on July 30, 2012*)

The chemical composition and morphology of M_7C_3 eutectic carbides in 19 mass% Cr–2.8 mass% C white iron with up to 4.7 mass% V additions have been studied. Eutectic colonies are mainly composed of a very fine rod-like carbides at the center and become coarser rod-like or blade-like with increased distance from the center. The volume fraction, size and distribution of rod-like and blade-like carbides in the eutectic colonies are changing with increasing vanadium content in the alloys. The formation of the eutectic colonies of different morphology is the consequence of the segregation of alloying elements in the alloy melt, which was confirmed by EDS analysis of the chemical composition of carbides. Three different compositions of M_7C_3 carbides were found in all tested alloys. The main difference between them is in the amount of chromium and iron and in the degree of their replacement by vanadium. Due to different melt composition in particular zones, the constitutional undercooling, and subsequently the growth rate, will be different, which will induce the formation of eutectic colonies of different morphologies.

KEY WORDS: Fe–Cr–C–V alloys; chemical composition of M_7C_3; morphology of M_7C_3; constitutional undercooling; growth rate.

1. Introduction

White cast irons have been widely used for abrasion resisting applications, so the primary characteristic of this alloy is a good abrasion resistance, and a modest resistance to brittle fracture. Most improvements in abrasion resistance are accompanied by lower toughness caused by higher content of eutectic carbide.[1–3] Studies concerning the effect of eutectic carbides on the abrasive wear resistance of high chromium white cast irons have been focused primarily on the volume fraction of carbides,[4,5] or their sizes, as it was estimated that fine carbides were more beneficial to the wear resistance than coarse ones.[5–7] There is a significant amount of work regarding the improving impact of carbidizing elements such as tungsten,[8] niobium,[9–11] vanadium,[5,9,12–16] titanium,[7,9,15,17] and boron[18] on the properties of high chromium white iron. Vanadium appeared to be of special interest, due to its double effects, on both the matrix structure and stereological characteristics of carbides.

Dependent upon the chemical composition of the melt, solidification of high chromium white cast irons begins with the formation of primary phase (*i.e.* austenite in hypoeutectic alloys, or M_7C_3 in hypereutectic alloys), and ends with the formation of the eutectic phase. Alloy with eutectic composition solidifies with eutectic cellular structure (γ + M_7C_3).[2,6,19–21] The hexagonal $(Cr,Fe)_7C_3$ carbides grow as rods and blades, with the fastest [0001] growth direction, and form a continuous network within each eutectic colony.[1,4,22] In the casting these eutectic colonies are oriented perpendicular to the mold surface in the columnar region, but have a random orientation in the equiaxed zone.[19,20,23]

The main goal of this work is to examine the influence of vanadium addition on the chemical composition and morphology of M_7C_3 eutectic carbides in high chromium white cast iron. The presented results are part of the research concerning the possibility of improving the properties of chromium white cast iron alloying with vanadium, particularly impact toughness, which is used for grinding balls ore, coal, gravel, and cement. In the industrial conditions, the balls of diameters 20–50 mm are cast in sand molds (Shell procedure), whereas balls of diameters 60–110 mm are cast in water-cooled permanent molds. Due to relatively high cooling rates the non-equilibrium solidification conditions occur. In order to provide the same casting conditions (similar to those in the industrial conditions) for all investigated alloys, *i.e.* to be able to monitor only the influence of vanadium (where the influence of other factors could be disregarded) on the changes in microstructure, samples for microstructural characterization were cast in laboratory conditions.

2. Experimental Procedure

The chemical composition of tested alloys is listed in **Table 1**. The melting of various alloys has been conducted in induction furnace. Test samples for structural analysis have been cut from the cast bars (200 mm long and 30 mm in diameter) cast in the sand molds. The calculated cooling

* Corresponding author: E-mail: mirjanaf@tmf.bg.ac.rs
DOI: http://dx.doi.org/10.2355/isijinternational.52.2200

rate of tested samples is approximately 1°C s^{-1}.[12]

The microstructure was examined using conventional optical microscopy (OM), scanning electron microscopy (SEM) and transmission electron microscopy (TEM). Samples for optical microscope examinations were prepared using standard metallographic technique (etched with Murakami). The volume fraction of the eutectic carbides was determined using image analyzer. The morphology of M_7C_3 eutectic carbides was examined by a scanning electron microscope, JEOL 733-FCXA, using an accelerating voltage of 25 kV. For this examination, the polished samples were deep etched in a 10% HCl solution in methanol for 24 h then cleaned in an ultrasonic bath. The chemical composition of the eutectic carbides was determined using energy dispersive X-ray spectroscopy (EDS). Discs for TEM examinations were prepared by using a twin-jet electropolisher. These samples were examined at 200 kV in a JEOL-2000FX transmission electron microscope.

3. Results

The as-cast microstructure of examined hypoeutectic Fe–Cr–C–(V) type alloys consists of primary austenite dendrites and eutectic colonies composed of M_7C_3 carbides and austenite (**Fig. 1**). Increasing the vanadium content appeared to give finer eutectic carbide structures, as shown in Fig. 1. Using by the image analyzing technique it was found that the volume fraction of eutectic carbides increased from 31% in alloy with no vanadium to 35.5% in alloy containing 4.73 mass% V. **Figure 2** shows a part of the eutectic M_7C_3 carbide containing many twins.

The SEM micrographs of deep etched sample revealed that single M_7C_3 carbides in Fe–Cr–C alloy with no vanadium addition, were rod or blade shaped (**Fig. 3**), where the blades are basically consist of multiple rods (Fig. 3(d)). A larger number of long carbide rods within the eutectic colonies usually grow along their longitudinal axes (Fig. 3(a)). When viewed perpendicular to their fastest growth direction, the M_7C_3 carbides within the eutectic colonies are very fine rod-like at the center, but become coarser rod-like (Fig. 3(b)) or blade-like (Fig. 3(c)) with increasing distance from the center. In addition, eutectic colonies in which blades spread radially from the center are observed in the columnar

Table 1. Chemical composition of tested Fe–Cr–C–V alloys (mass%).

Alloy	C	P	S	Si	Mn	Mo	Cu	Ni	Cr	V
1	2.89	0.025	0.061	0.85	0.71	0.48	0.99	0.100	19.03	0.0012
2	2.92	0.026	0.063	0.87	0.76	0.45	1.02	0.099	19.01	0.12
3	2.92	0.025	0.061	0.85	0.75	0.43	1.01	0.098	19.04	1.19
4	2.87	0.024	0.063	0.87	0.73	0.44	1.01	0.099	18.92	2.02
5	2.91	0.027	0.061	0.84	0.73	0.44	1.00	0.096	19.05	3.28
6	2.93	0.026	0.062	0.83	0.74	0.43	1.01	0.098	19.07	4.73

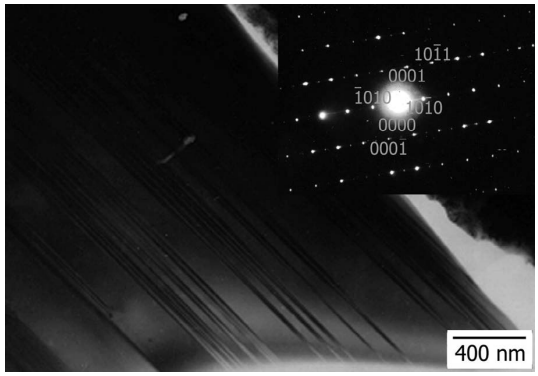

Fig. 2. TEM micrographs of Fe–Cr–C–V alloy containing 3.28%V showing hexagonal M_7C_3 eutectic carbide and selected-area diffraction pattern (in the corner) from the region in this micrograph.

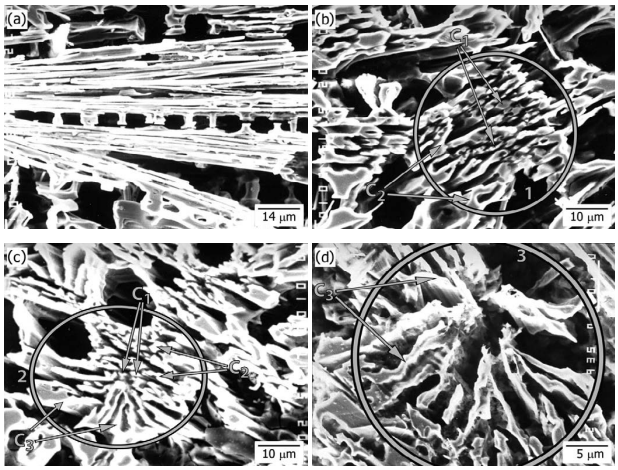

Fig. 3. SEM micrographs of deep etched sample showing morphology of M_7C_3 carbides in Fe–Cr–C alloy with no vanadium addition: (a) eutectic colonies consisting of a larger number of long M_7C_3 carbide rods which grow along their longitudinal axes; (b) and (c) eutectic colonies when viewed perpendicular to their fastest growth direction (mainly composed of very fine rod-like carbides in the center, becoming coarser rod-like (b) or blade-like (c) with increased distance from the centre), and (d) rosette-like eutectic colonies in which blade-like carbides are located radially from the centerer. Different morphologies of eutectic colonies are marked 1 to 3. M_7C_3 carbides of different compositions marked by arrows C_1 to C_3.

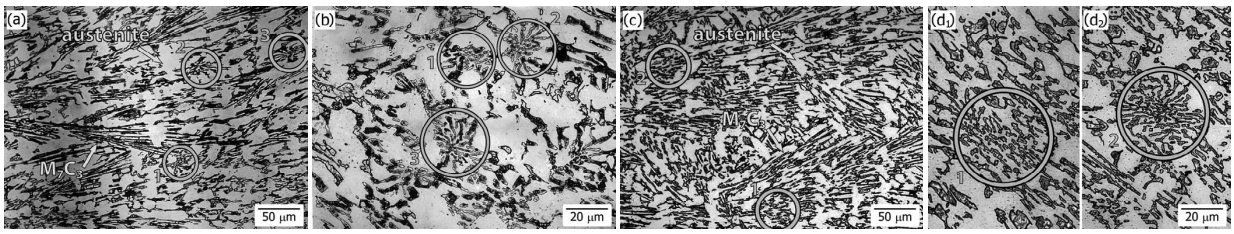

Fig. 1. Optical micrographs of Fe–Cr–C alloy ((a) and (b)) and Fe–Cr–C–V alloy containing 3.28% V ((c), (d_1) and (d_2)) in the columnar zone of as-cast structures (5 mm from the surface). Different morphologies of eutectic colonies are marked 1 to 3.

zone of this alloy (Fig. 3(d)).

In Fe–Cr–C–V type alloys the higher vanadium content was followed with increased number of carbide rods within the eutectic colonies, and, the rod or blade-like M_7C_3 carbides were finer (**Figs. 4** and **5**). It should be emphasized that in alloy with 3.28% vanadium, eutectic colonies with radially spreading blade shaped carbides were not observed (Fig. 5).

Results obtained by EDS analysis of the eutectic M_7C_3 carbides in the tested Fe–Cr–C–V alloys are given in **Table 2**. The carbon content was calculated by balancing with the other elements. As shown in Table 2, three different compositions of M_7C_3 carbides were found in all the tested alloys. The main difference between them has been recognized in various chromium and iron content. While Fe/Cr ratio of atomic fraction in Fe–Cr–C–V alloy containing 0.12% V is 0.71 for carbides of composition C_1, it is 0.99 for carbides C_2 and 1.31 for carbides of composition C_3. In C_1 and C_2 carbides of the alloy containing 1.19% V, vanadium substitutes chromium atoms in M_7C_3 carbides lattice, while in carbide of composition C_3, it substitutes iron atoms. The Fe/Cr ratio in this alloy is 0.79, 1.03 and 1.26 for carbides of composition C_1, C_2 and C_3, respectively. In alloys containing 3.28% V and 4.73% V, chromium and iron atoms have been substituted by vanadium in all three different compositions of eutectic carbides. In cases of C_1 and C_2 carbies greater number of chromium atoms were substituded by vanadium, while in carbides C_3 greater number of iron atoms have been substituted.

The eutectic colony consists of carbides of different compositions in all examined alloys (Figs. 3–5). Blade-like carbides predominantly show C_3 composition.

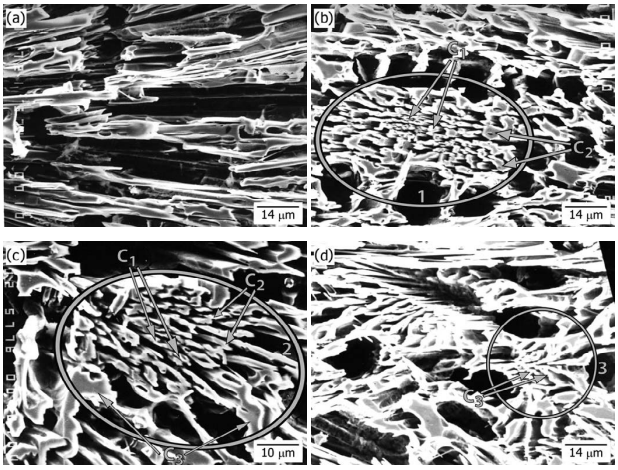

Fig. 4. SEM micrographs of deep etched sample showing morphology of M_7C_3 carbides in Fe–Cr–C–V type alloy containing 1.19% V: (a) eutectic colonies consisting of a larger number of long M_7C_3 carbide rods which grow along their longitudinal axes; (b) and (c) eutectic colonies when viewed perpendicular to their fastest growth direction (mainly composed of very fine rod-like carbides in the center, becoming coarser rod-like (b) or blade-like (c) with increased distance from the centre), and (d) rosette-like eutectic colonies in which blade-like carbides are located radially from the centerer. Different morphologies of eutectic colonies are marked 1 to 3. M_7C_3 carbides of different compositions marked by arrows C_1 to C_3.

4. Discussion

In the tested Fe–Cr–C–V type alloys the solidification starts with the formation of austenite dendrites. In the course of primary γ-phase growth, the composition of the remained liquid was changing. Due to limited solubility of carbon, chromium and vanadium in the austenite, these elements accumulated in front of the progressing solid-liquid interface. At temperature lower than liquidus temperature during the eutectic reaction that takes place, in local areas enriched in vanadium, eutectic composed of vanadium reach M_6C_5 carbide and austenite was developed. This effect was considered previously in details.[12] As the temperature falls and solidification progresses, primary austenite dendrites reject solute (mainly carbon, chromium and vanadium) in to the remaining liquid until the eutectic composition is reached and the monovariant eutectic reaction ($L \rightarrow \gamma + M_7C_3$) takes place. From the melt remained in interdendritic regions the coupled M_7C_3/γ (faceted-nonfaceted) eutectic was forming.

Irregular eutectic structures are developed when a nonfaceted phase is coupled with a faceted phase. In such eutectics, local morphological adjustment of interphase spacing is severely encumbered by the limited branching ability of the highly anisotropic faceted phase containing planar defects. Thus, the spatially non-uniform or irregular structure that evolves during faceted-nonfaceted eutectic solidification is inherently three-dimensional, where the relationship between the growth mechanisms of the faceted phase and the complex non-isothermal interface structure gives rise to a more diverse range of solidification microstructures than that exhibited by regular eutectics.[24,25] It has been reported[25] that solute elements, even in trace amounts, may have a strong influence on eutectic growth morphology.

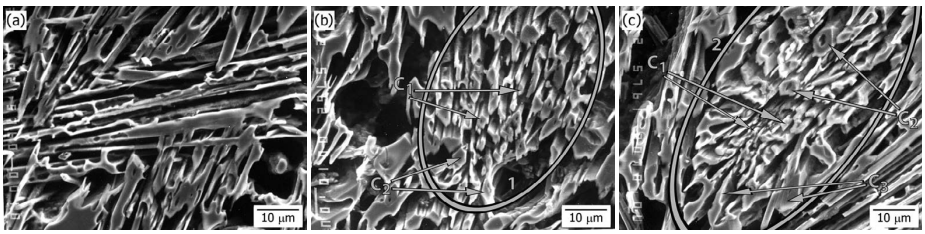

Fig. 5. SEM micrographs of deep etched sample showing morphology of M_7C_3 carbides in Fe–Cr–C–V type alloy containing 3.28% V: (a) eutectic colonies consisting of a larger number of long M_7C_3 carbide rods which grow along their longitudinal axes; (b) and (c) eutectic colonies when viewed perpendicular to their fastest growth direction (mainly composed of very fine rod-like carbides in the center, becoming coarser rod-like (b) or blade-like (c) with increased distance from the centre). Different morphologies of eutectic colonies are marked 1 and 2. M_7C_3 carbides of different compositions marked by arrows C_1 to C_3.

Table 2. Chemical composition of M_7C_3 eutectic carbide in Fe–Cr–C–V alloys.

Alloy	M_7C_3	Chemical composition of M_7C_3* (mass%)								
		C	Si	Mn	Mo	Cu	Cr	Fe	V	Formula
1	C_1	8.17±0.38	0.028±0.008	0.673±0.06	0.557±0.13	0.032±0.016	53.36±0.94	38.07±0.82	–	$Cr_{4.2}Fe_{2.8}C_3$
	C_2	8.55±0.27	0.033±0.009	0.548±0.08	0.674±0.15	0.047±0.019	45.44±0.76	44.68±0.67	–	$Cr_{3.6}Fe_{3.3}C_3$
	C_3	8.43±0.42	0.019±0.005	0.659±0.07	0.494±0.09	0.053±0.022	39.77±1.01	50.11±0.93	–	$Cr_{3.2}Fe_{3.8}C_3$
2	C_1	8.35±0.30	0.031±0.006	0.781±0.07	0.595±0.10	0.020±0.015	53.12±0.57	37.91±0.43	0.111±0.012	$Cr_{4.2}Fe_{2.8}C_3$
	C_2	8.18±0.44	0.014±0.007	0.487±0.07	0.538±0.08	0.045±0.024	45.88±1.02	45.29±0.87	0.076±0.009	$Cr_{3.6}Fe_{3.3}C_3$
	C_3	8.67±0.38	0.028±0.007	0.663±0.06	0.686±0.12	0.038±0.018	38.87±0.76	51.18±0.58	0.078±0.008	$Cr_{3.1}Fe_{3.8}C_3$
3	C_1	8.23±0.41	0.011±0.007	0.667±0.08	0.541±0.07	0.049±0.016	48.43±0.88	38.13±0.54	3.63±0.015	$Cr_{3.8}Fe_{2.8}V_{0.3}C_3$
	C_2	8.48±0.28	0.032±0.005	0.535±0.06	0.672±0.14	0.029±0.015	42.72±0.46	44.22±0.43	2.76±0.009	$Cr_{3.4}Fe_{3.3}V_{0.2}C_3$
	C_3	8.41±0.35	0.055±0.006	0.671±0.09	0.479±0.11	0.048±0.027	38.72±0.84	48.93±0.66	2.75±0.018	$Cr_{3.1}Fe_{3.6}V_{0.2}C_3$
5	C_1	8.56±0.32	0.045±0.009	0.461±0.07	0.451±0.08	0.059±0.023	45.46±0.93	34.54±0.65	10.62±0.022	$Cr_{3.6}Fe_{2.6}V_{0.8}C_3$
	C_2	8.62±0.37	0.027±0.007	0.675±0.05	0.564±0.12	0.037±0.018	38.53±0.52	43.92±0.48	7.74±0.013	$Cr_{3.1}Fe_{3.2}V_{0.6}C_3$
	C_3	8.28±0.44	0.029±0.004	0.427±0.07	0.448±0.07	0.056±0.022	35.52±0.78	46.01±0.62	8.35±0.015	$Cr_{2.8}Fe_{3.4}V_{0.7}C_3$
6	C_1	8.44±0.46	0.016±0.008	0.585±0.08	0.671±0.15	0.061±0.025	43.16±0.67	32.97±0.52	14.19±0.028	$Cr_{3.4}Fe_{2.4}V_{1.1}C_3$
	C_2	8.14±0.33	0.031±0.005	0.643±0.06	0.451±0.12	0.048±0.017	38.03±0.83	40.92±0.83	11.79±0.017	$Cr_{3.0}Fe_{3.0}V_{0.9}C_3$
	C_3	8.37±0.38	0.013±0.008	0.591±0.07	0.493±0.08	0.053±0.017	34.19±0.58	45.24±0.45	11.53±0.024	$Cr_{2.7}Fe_{3.4}V_{0.8}C_3$

*: The values are based on an average of thirty different measurements per each of three different chemical compositions of M_7C_3 eutectic carbide in all tested alloys.

In the columnar zone of as-cast structures, the eutectic carbides are usually aligned so that the long axis of the carbide rods is parallel with the direction of heat flow (*i.e.* perpendicular to the cast surface), forming a highly anisotropic morphology. The formation of eutectic colonies of different morphologies is assumed to be related to the segregation of alloying elements in the melt. That is confirmed by EDS analysis which indicates different M_7C_3 carbide compositions (Table 2). During solidification, solute segregation will influence nucleation and growth kinetics through its influence on constitutional undercooling (the constitutional undercooling of a particular phase is dependent on the liquidus and/or eutectic temperature which, in turn, is dependent on the local liquid composition). Due to different melt composition in particular regions, the constitutional undercooling and also the growth rate are different and the formation of eutectic colonies with different morphologies will be induced (Figs. 1, 3, 4 and 5). According to solidification theory,[24] for a hypoeutectic alloy composition, the alloy liquidus is much higher than the eutectic temperature. Thus the corresponding primary phase is highly constitutionally undercooled, due to the long-range boundary layer built up ahead of the solid-liquid interface in this case, and tends to grow faster than the eutectic. Consequently, primary phase will destabilize the solid-liquid interface. At the time when eutectic nucleation and growth occur, the conditions in the melt will in part be imposed by the characteristics of the previous reaction.[25] Since it can be assumed that thermal conditions, such as thermal gradient and cooling rate, are the same, the morphology of the eutectic growth front will depend on melt composition in particular zones. In the regions with a smaller content of alloying elements, the rosette-like eutectic colonies in which carbides are located radially from the center will be formed (Figs. 1(b), 3(d) and 4(c)), whereas in regions of enriched melt, the formation of eutectic colonies consisting of a larger number of long M_7C_3 carbide rods will be favored (Figs. 1(a), 1(b), 3(a), 4(a) and 5(a)).

In each of tested Fe–Cr–C–(V) type alloys, three different compositions of M_7C_3 carbides with different the Fe/Cr ratio of atomic fraction (Table 2) have been found, as the consequence of the composition inhomogeneity of the melt. However, in the earlier studies[9,19,26–28] it has been noticed that Fe/Cr ratio in eutectic carbides depends on carbon content in alloys with the same chromium content (hypoeutectic, eutectic and hypereutectic type alloy) or on the cooling rate. Doğan *et al.*[19] did observe that while the Fe/Cr ratio of atomic fraction in the M_7C_3 carbide of hypoeutectic and eutectic high chromium white iron with 15% Cr is approximately 1, it is 1.3 in 15% Cr hypereutectic iron. Jacuinde[9] has found in the study of iron containing 16.9% Cr, 2.58% C and 1.98% V that for higher cooling rate Fe/Cr ratio is 1.36, and that for slower cooling rate Fe/Cr ratio is 0.97.

In all examined alloys, the morphology of the eutectic carbides vary from the center to the edge of eutectic colonies marked 1 and 2 in Figs. 3–5. The rod shaped carbides are finer at the center of the eutectic colony and become coarser rod-like or blade-like with increased distance from the center (Figs. 3–5), as indicates that eutectic solidification begins at the center with a certain undercooling and proceeds radially outward. As solidification progresses, the constitutional undercooling decreases, and thus the rod-like or blade-like carbides that form during the later stages of solidification are coarser. This can be explained by the fact that, during M_7C_3/γ eutectic growth, the solute atoms (as carbon, chromium and vanadium), which are rejected by one phase, are usually needed for the growth of the other. Therefore, lateral diffusion along the solid-liquid interface perpendicular to the growth direction, will become dominant and effectively decreases the solute build-up (ΔC) ahead of both phases. This lateral diffusion causes the interphase spacing λ in the eutectic structure to be decreased.

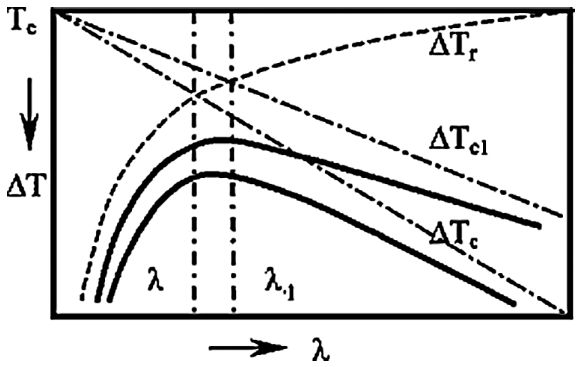

Fig. 6. Adjustment of interphase spacing during eutectic growth.[24,29)]

However, as λ decreases, an opposing force (capillary effect), which arises from the increased energy associated with the increased curvature of the solid/liquid interface, comes into effect. As shown in **Fig. 6**, the diffusion effect can be expressed in terms of a constitutional undercooling (ΔT_c) while the latter can be expressed in terms of a curvature undercooling (ΔT_r).[24,29)] The sum of the solute (ΔT_c) and curvature (ΔT_r) undercoolings must therefore equal the interface undercooling, ΔT. Both undercoolings vary with λ in opposite ways: ΔT_c, which is proportional to ΔC (the driving force for solute diffusion) increases with λ, while ΔT_r decreases. The interphase spacing in the eutectic structure is eventually established by the equilibrium between an attractive force arising from the diffusion effect and a repulsive force arising from the curvature effect. Decrease in growth rates will shift ΔT_c to ΔT_{c1} without changing the ΔT_r curve, leading to a higher spacing value, λ_1. It is also evident from Fig. 6 that for small values of λ, eutectic growth is controlled by capillary effects ($\Delta T_r > \Delta T_c$), while diffusion is the limiting process at large spacing values.[24,29)] With increasing λ values the size of M_7C_3 carbides increases.

In the case of eutectic colonies marked 3 in Figs. 3(d) and 4(d), eutectic grows uniformly in all directions and finally a rosette-like structure is obtained.

The morphology of particular M_7C_3 carbides in Fe–Cr–C–V alloys does not significantly change with increasing vanadium content. These carbides are rod or blade shaped. The volume fraction, size and distribution of rod-like and blade-like carbides in the eutectic colonies are changing with increasing vanadium content in the examined alloys (Figs. 4 and 5). The rod type morphology of eutectic carbides is more dominant in Fe–Cr–C–V alloys with higher content of vanadium. These changes in morphology can be explain by the fact that in alloy with higher vanadium content, due to higher concentration of vanadium in the melt, and subsequently larger constitutional undercooling, the growth rate is faster than in alloys with lower vanadium content, under the same cooling conditions.

5. Conclusions

Solidification structure observations in Fe–Cr–C–(V) alloys with different vanadium content were presented. Eutectic colonies of different morphologies are observed in all examined alloys.

Eutectic colonies are mainly composed of very fine rode-like carbides in the center of the colonies, becoming coarser rod-like or blade-like with increased distance from the centre. The volume fraction, size and distribution of rod-like and blade-like carbides in the eutectic colonies are changing with increasing vanadium content in the tested alloys. It occured in a smaller extent in the structures of alloys containing up to 2.02% V, with eutectic colonies in which blade shaped carbides are spreading radially from the centre. The rod type morphology of eutectic carbides is more dominant in Fe–Cr–C–V alloys with higher content of vanadium.

The formation of eutectic colonies of different morphologies is the consequence of the segregation of alloying elements in the alloy melt. The EDS analysis confirmed the presence of three different chemical compositions of M_7C_3 carbides in all tested alloys. The main difference between them is in the amount of chromium and iron, and in the degree of their replacement by vanadium. Due to different melt composition in particular zones, the constitutional undercooling, and subsequently the growth rate, are different, which will induce the formation of eutectic colonies of different morphologies.

REFERENCES

1) J. Dodd and J. L. Parks: *Met. Forum*, **3** (1980), 3.
2) C. P. Tabrett, I. R. Sare and M. R. Ghomashchi: *Int. Mater. Rev.*, **41** (1996), 59.
3) A. Wiengmoon, T. Chairuangsri and J. T. H. Pearce: *ISIJ Int.*, **44** (2004), 396.
4) S. D. Carpenter, D. Carpenter and J. T. H. Pearce: *Mater. Chem. Phys.*, **85** (2004), 32.
5) A. Wiengmoon, T. Chairuangsri, A. Brown, R. Brydson, D. V. Edmonds and J. T. H. Pearce: *Acta Mater.*, **53** (2005), 4143.
6) G. Laird II and Ö. N. Doğan: *Int. J. Cast Metal. Res.*, **9** (1996), 83.
7) A. Bedolla-Jacuinde, R. Correa, J. G. Quezada and C. Maldonado: *Mater. Sci. Eng. A*, **398** (2005), 297.
8) S. H. Mousavi Anijdan, A. Bahrami, N. Varahram and P. Davami: *Mater. Sci. Eng. A*, **454–455** (2007), 623.
9) A. Bedolla-Jacuinde: *Int. J. Cast Metal. Res.*, **13** (2001), 343.
10) A. Sawamoto, K. Ogi and K. Matsuda: *J. Jpn. Inst. Met.*, **49** (1985), 475.
11) C. R. Loper and H. K. Baik: *AFS Trans.*, **97** (1989), 1001.
12) M. Filipovic, Z. Kamberovic and M. Korac: *Mater. Trans.*, **52** (2011), 386.
13) M. Radulovic, M. Fiset, K. Peev and M. Tomovic: *J. Mater. Sci.*, **29** (1994), 5085.
14) M. Filipovic, E. Romhanji, Z. Kamberovic and M. Korac: *Mater. Trans.*, **50** (2009), 2488.
15) J. Wang, R. L. Zuo, Z. P. Sun, C. Li, K. K. Liu, H. S. Yang, B. L. Shen and S. J. Huang: *Mater. Charact.*, **55** (2005), 234.
16) M. Filipovic and E. Romhanji: *Wear*, **270** (2011), 800.
17) X. Wu, J. Xing, H. Fu and X. Zhi: *Mater. Sci. Eng. A*, **457** (2007), 180.
18) Z. Liu, Y. Li, X. Chen and K. Hu: *Mater. Sci. Eng. A*, **486** (2008), 112.
19) Ö. N. Doğan, J. A. Hawk and G. Laird II: *Metall. Mater. Trans. A*, **28** (1997), 1315.
20) Ö. N. Doğan: *Scr. Mater.*, **35** (1996), 163.
21) A. Bedolla-Jacuinde, B. Hernández and L. Béjar-Gómez: *Z. Metallkd.*, **96** (2005), 1380.
22) S. D. Carpenter, D. Carpenter and J. T. H. Pearce: *J. Alloy. Compd.*, **494** (2010), 245.
23) Ö. N. Doğan, G. Laird II and J. A. Hawk: *Wear*, **181–183** (1995), 342.
24) W. Kurz and D. J. Fisher: Fundamentals of Solidification, Trans Tech Publication, Switzerland, (1984), 97.
25) M. Asta, C. Beckermann, A. Karma, W. Kurz, R. Napolitano, M. Plapp, G. Purdy, M. Rappaz and R. Trivedi: *Acta Mater.*, **57** (2009), 941.
26) K. Ogi, Y. Matsubara and K. Matsuda: *AFS Trans.*, **89** (1981), 197.
27) C. Cetinkaya: *Mater. Design*, **27** (2006) 437.
28) X. Zhi, J. Xing, Y. Gao, H. Fu, J. Peng and B. Xiao: *Mater. Sci. Eng. A*, **487** (2008), 171.
29) L. Lu, H. Soda and A. McLean: *Mater. Sci. Eng. A*, **347** (2003), 214.